Available online at www.sciencedirect.com
ScienceDirect
International Journal of Multiphase Flow 32 (2006) 1311–1325
International Journal of Multiphase Flow
www.elsevier.com/locate/ijmulflow

Motion of singles bubbles moving under a slightly inclined surface through stationary liquids

A.L. Perron, L.I. Kiss *, S. Poncsák

Département des sciences appliquées, Université du Québec à Chicoutimi, 555 boulevard de l'Université, Chicoutimi, Québec, Canada G7H 2B1

Received 3 March 2006; received in revised form 17 July 2006

Abstract

The influence of the liquid properties on the dynamical bubble shape and on the bubble motion has been investigated for bubbles moving under a downward facing inclined surface. The Morton number Mo varied from 2.59×10^{-11} to $2.52 \times 10^{+01}$. The Bond number Bo covered the range from 10 to 150 and the surface inclination angle θ was varied from 2° to 6°. To cover the wide range of Mo, several liquids such as glycerine, propanediol, water and isopropanol were used. The results have shown that the relation $Fr = Fr(Bo, Mo, \theta)$ is not adequate to describe the bubble motion, where Fr is the terminal Froude number. The choice of the terminal Reynolds number Re as the dependent parameter, allowed the clarification of the role of the Morton number on the bubble motion. At a given Bond number, the bubble Reynolds number decreases monotonously with the Morton number. Furthermore, an empirical correlation $Re = Re(Bo, Mo, \theta)$ is given that can be readily used in the mathematical modelling of bubble laden flows under solids.

Keywords: Bubble shape; Downward facing surface; Terminal velocity; Morton number

1. Introduction

Bubbles are encountered in many industrial processes. Several works have been devoted to the prediction of their motion in extended as well as in bounded media. Vertical and inclined tubes are examples of finite domains. In certain situations, like in production of aluminium or in nuclear engineering, bubbles move under an inclined surface. The knowledge of their motion is essential to increase the understanding of these complex industrial processes. The number of articles published on the rise of bubbles under inclined surfaces is very small compared to the number of articles devoted to the movement of bubbles through tubes. Masliyah et al. (1994) studied the rise velocity of very small bubbles of air along an inclined surface in water–glycerine solutions. The bubble volume V varied from 0.0026 cm^3 to 0.013 cm^3 and the inclination from 35° to 90° from the horizontal. It was found that the terminal velocity increases monotonously as the inclination angle is

* Corresponding author. Tel.: +1 418 545 5011; fax: +1 418 545 5012.
E-mail address: lkiss@uqac.ca (L.I. Kiss).

0301-9322/$ - see front matter
doi:10.1016/j.ijmultiphaseflow.2006.08.001

increased towards the vertical. They did not find a critical inclination angle at which the velocity is maximal. Perron et al. (2006a) studied the motion of single bubbles in the wetting regime under a slightly inclined surface. The air–water–Plexiglas system was only driven by the gravity force. The bubble volume varied from 0.3 cm^3 to 9 cm^3 and the inclination angle was varied between 2° and 10° from the horizontal. The results showed that the rise velocity does not increase monotonously with the bubble volume at a given surface inclination. It was found that, at a given inclination, there may exist four different sub-regimes each characterized by a specific bubble shape. The terminal velocity increased as the inclination angle was increased and its influence was more considerable at both small bubble volumes and low inclination angles. Maxworthy (1991) studied the motion of large bubbles moving under an inclined plate through an air–water gravity driven system. The bubble volumes varied from 5 cm^3 to 60 cm^3 at intervals of 5 cm^3 and the surface inclination was varied from 5° to 90° from the horizontal. The slope was increased by steps of 5° except for the values of 55°, 65° and 75°. It was found that the terminal velocity of a bubble increases monotonously with the bubble volume and the rise velocity (terminal velocity) reaches a maximal value at an inclination of about 50°. In all experiments, the bubble motion was controlled principally by the inertia. Except the work of Masliyah et al. (1994), which treats of very small bubble volumes, data referring to bubble rising under an inclined wall are only available for air–water system. The purpose of this work is to study the motion of bubbles rising under a slightly inclined surface through stationary liquids. Before presenting our results, we discuss the effects of the liquid properties on the rise of bubbles in infinite and finite media.

The influence of the fluid properties on the motion of a bubble is complex and not evident to describe. For example, to isolate the effect of the viscosity on the bubble motion experimentally, we should find two non-toxic liquids with nearly the same density and surface tension but with different viscosities. To overcome this difficulty many authors used the Morton number defined as

$$Mo = \frac{g v_L^4 \rho_L^3}{\sigma^3} \tag{1}$$

to describe the working liquid. Here, ρ_L, v_L and σ are the density, the kinematic viscosity and the surface tension of the working liquid, respectively. The physical properties of the gas phase are neglected. Then, the Morton number is solely dependent of the physical properties of the liquid. Hartunian and Sears (1957) studied the instability of gas bubbles rising in various liquids. Their results suggest that there are two separate criteria to describe the onset of instability depending of the nature of the working fluid. The bubbles rising at a Reynolds number less than 202 through a high viscosity fluid or impure liquid are invariably stable whereas bubbles rising at $Re > 202$ in a pure liquid, relatively inviscid, are stable until they reach a critical Weber number of 1.26. The terminal Reynolds number and the Weber number are expressed as

$$Re = \frac{u_T d}{v_L}, \tag{2}$$

$$We = \frac{\rho_L u_T^2 d}{\sigma}, \tag{3}$$

where u_T is the bubble terminal velocity and d is the equivalent diameter of the bubble defined as

$$d = \left(\frac{6V}{\pi}\right)^{1/3}, \tag{4}$$

where V is the bubble volume. The terminal Reynolds number represents the ratio of hydrodynamical forces or inertia to the viscous forces while the Weber number is the ratio of the inertia to the surface tension forces. Zukoski (1966) studied the influence of viscosity, surface tension, and inclination angle on the motion of long bubbles in closed tubes. The tube diameters have been determined in order that the surface tension force play a significant role on the movement of the long bubbles. It has been found that in the case of a vertical tube, the effect of viscosity is negligible if the Re based on the tube diameter is greater than 200. In this situation, the results showed that the Froude number reached a limiting value as the Bond number increased. In the case of rising bubble through an inclined tube, the Froude number continues to increase with the Bond number. For a moving bubble bounded within a tube, the Bond and the Froude numbers are defined by

$$Bo = \frac{\rho_L g a^2}{\sigma}, \tag{5}$$

$$Fr^* = \frac{u_T}{\sqrt{ga}}, \tag{6}$$

respectively, where a is the tube diameter. Maneri and Zuber (1974) investigated the motion of plane bubbles as function of tank width, tank spacing, bubble volume, inclination and fluid properties. For vertical plane bubbles the latter did not affect the terminal velocity while in the case of plane bubbles rising at inclination, the terminal velocity was higher in methanol than in water for a given bubble volume. Bhaga and Weber (1981) studied the motion of single bubbles rising through unbounded viscous liquids. The working liquid was sucrose and the Mo varied from 7.4×10^{-04} to 850. They measured the bubble terminal velocity, characterized the bubble shape and visualised the bubble wake by using the hydrogen bubble tracer technique. They observed that for $Mo > 4 \times 10^{-03}$, the drag coefficient and bubble shape were uniquely dependent of the Reynolds number. Weber and Alarie (1986) measured the terminal velocity of extended bubbles in inclined tubes through different liquids. The Morton number was varied from 2.2×10^{-11} to $1.5 \times 10^{+04}$. The authors presented their data in term of the Froude number as function of the Bond and Morton numbers and of the inclination angle. For the influence of the fluid properties on the motion of bubbles, they observed the same tendency as Zukoski (1966). Maxworthy et al. (1996) studied the vertical rise of an unbounded bubble in water–glycerine solutions. The value of the Morton number varied from 7.7×10^{-12} to 78. They found several new scaling regimes and discussed the dynamical processes that might govern each of them. Their results showed also the well-known tendencies that for highly viscous liquids, the surface tension regime does not exist and when the movement of a bubble is controlled by the inertia (spherical-cap regime), the terminal velocity is not influenced by the liquid properties.

Tsao and Koch (1997) studied experimentally the motion of tiny single bubbles rising under an inclined solid plate. The bubble volume was varied from 5.23×10^{-4} to 1.43×10^{-3} cm^3 while the inclination angle ranging from 10° to 85° to the horizontal. It was observed that when the inclination angle was less than 55° corresponding to $We = 0.4$, the bubble glides steadily under the plate. The authors mentioned that to maintain the wetting or in other words lubrication film, a hydrodynamic lift force must exist to balance the perpendicular component (to the plate) of the buoyancy force. By using the results of Antal et al. (1991), they concluded that the contribution of the inertial lift is too small. Thus the lift was attributed to the viscous stress generated in the wetting film. At higher inclination angles, they observed a periodic bouncing motion of the bubble against the inclined wall without any loss of amplitude. The authors explained this phenomenon by a transformation of the gravitational potential (as the bubble rises along the plate) into kinetic and surface deformation energy. DeBisschop et al. (2002) studied numerically the motion of a two-dimensional bubble in an inclined channel by using the boundary integral method and the Stokes equations for the fluids. They found that the terminal velocity increases monotonically with the inclination angle. The results have shown that for inclination angles ranging from 30° to 40° the bouncing motion appeared with possibly decreasing of amplitude. For slopes greater than 40° until the vertical, the bubbles bounced once. Furthermore, the thickness of the wetting film increased with the Bond number as well as with the inclination angle. Norman and Miksis (2005a) investigated numerically the dynamics of a small two-dimensional gas bubble initially located at the center of an inclined channel. The values of the Bond and Reynolds numbers were less than 10 and 100, respectively. The inclination angle of the channel was varied from 30° to 90° to the horizontal. At low slopes, they obtained steady state solutions for the bubble rise. Above a critical inclination, their results showed the periodic bouncing motion observed experimentally by Tsao and Koch (1997). In a second paper, Norman and Miksis (2005b) realized a computational work concerning the rise of small bubble initially attached to the upper wall of an inclined channel. The limits of the Bond and the Reynolds numbers as well as the inclination angle were nearly the same than in their previous study (Norman and Miksis, 2005a). At small values of these numbers, steadily rising bubbles have been computed. For a given Bo, the effect of increasing Re was to create periodic oscillations of the bubble shape. At large Re or Bo, detachment of the bubble from the wall as well as bubble break-up has been computed.

In the series of experiments presented here, the influence of the physical properties of working liquid on certain characteristic parameters such as the average geometrical aspect ratio as well as the bubble terminal velocity is investigated.

2. Experiment

A schematic diagram of the experimental setup is shown in Fig. 1. The length, width and depth of the Plexiglass tank were 1.20, 0.34 and 0.34 m, respectively. The solid surface was represented by a Plexiglas plate 1 cm thick, 16 cm wide and 90 cm long fixed on the tank sides by two pivots. The experimental setup allows surface inclination angle up to 10°. In this work, the series of experiments have been carried out at inclination angles of 2°, 4°, 6° and 8°. The bubbles were generally created directly under the surface, behind a movable barrier for large bubbles, while in certain cases the bubbles were generated in an inverted cup. The bubbles were then released either by moving the mechanical barrier very slowly to avoid the acceleration of the fluid around the bubble or by simply rotating the cup in the other case. With both techniques, the bubble volumes were generally varied from 0.1 to 10 cm^3. To obtain the trajectory of the bubble, its instantaneous velocity, shape and terminal velocity u_T, a track-mounted high-speed digital camera was used to follow the moving bubble. The recording rate depended on the bubble volume as well as on the nature of the working liquid. A transparent grid (5 mm/division) was placed over the plate in order to identify the position of the bubble as a function of time. Each experiment was repeated three times. The maximal difference concerning the terminal velocity was 6% while it was 8% for the time-averaged aspect ratio. For more details about the experimental setup and the methodology (Perron et al., 2006a).

In the present work, the effects of three different pure liquids (excluding distilled water) and their aqueous solutions on the bubble motion are investigated. The liquids are isopropanol, propanediol and glycerine. To change the Morton number of the pure liquids we have used two different ways. The isopropanol and the propanediol have been diluted with water while the glycerine has been heated. Densities of the mixtures generated from the two first liquids were measured with a pycnometer, surface tension with a du Nouy ring setup and viscosities with capillary viscometers. These parameters were measured three times for each concentration and the averaged results are presented in Tables 1 and 2. For the glycerine, available data were taken from the literature while the unknown were measured and presented in Table 3. In this work, some earlier results

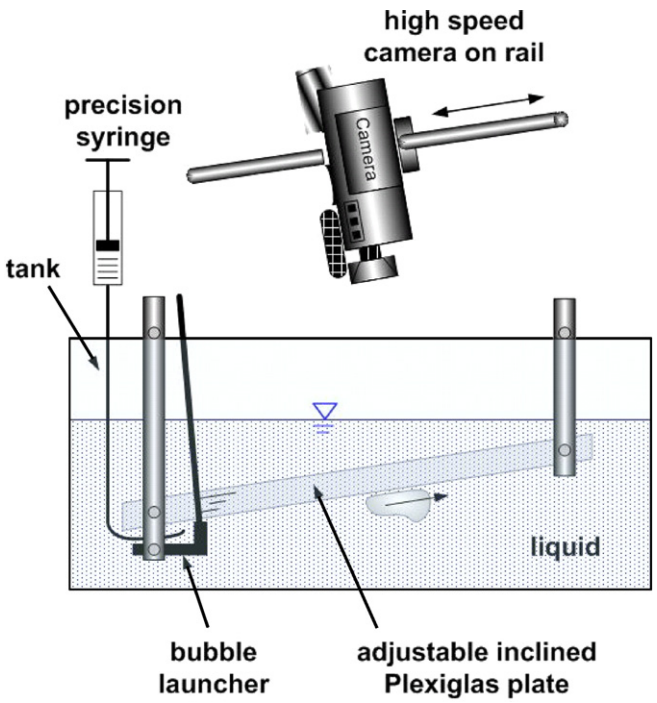

Fig. 1. Schematic of experimental apparatus.

Table 1
Physical properties of the propanediol–water solutions and the values of the Morton number

	Propanediol (% by wt)	Temperature (°C)	Surface tension (N/m)	Density (kg/m^3)	Viscosity (m^2/s)	*Mo*
1	99.5	20	0.0406	1034.7	4.98×10^{-05}	9.97×10^{-04}
2	75	20	0.0450	1040.0	1.67×10^{-05}	9.34×10^{-06}
3	50	20	0.0493	1035.3	6.67×10^{-06}	1.79×10^{-07}
4	25	20	0.0520	1015.3	2.52×10^{-06}	2.96×10^{-09}

Table 2
Physical properties of the isopropanol–water solutions and the values of the Morton number

	Isopropanol (% by wt)	Temperature (°C)	Surface tension (N/m)	Density (kg/m^3)	Viscosity (m^2/s)	*Mo*
5	99.5	20	0.0243	781.5	3.07×10^{-06}	2.89×10^{-08}
6	75	20	0.0266	844.4	3.89×10^{-06}	7.17×10^{-08}
7	50	20	0.0282	905.0	4.19×10^{-06}	1.00×10^{-07}
8	25	20	0.0318	957.6	2.86×10^{-06}	1.80×10^{-08}

Table 3
Physical properties of the glycerine and the values of the Morton number as function of the temperature

	Glycerine (% by wt)	Temperature (°C)	Surface tension (N/m)	Density (kg/m^3)	Viscosity (m^2/s)	*Mo*
9	99.5	22	0.0623	1257.3	7.48×10^{-04}	$2.52\times10^{+01}$
10	99.5	31	0.0619	1252.1	3.67×10^{-04}	$1.47\times10^{+00}$
11	99.5	41	0.0615	1246.2	1.77×10^{-04}	8.01×10^{-02}
12	99.5	50	0.0611	1240.3	9.67×10^{-05}	7.18×10^{-03}

obtained by the authors (Perron et al., 2006a) are also presented. These results concern the bubble motion through water where the Morton number is 2.59×10^{-11}.

Here, the emphasis was put on the determination of certain characteristic parameters of the bubble motion such as the terminal velocity u_T as well as the averaged aspect ratio r. Although the instantaneous velocity was computed at each time step, it was only used to determine the onset of the steady state regime. We consider that the steady state regime is reached when the instantaneous velocity oscillates around a mean value. The acceleration period in low-Morton-number liquids was generally below 1 s, while it exceeded slightly 1 s in high-Morton-number liquids. The transition period being short, – less than 1–10% of the total duration of observation – sufficient time was left to sample several points in the steady regime.

The paths (observed in the plane of the solid surface) of all the bubbles presented in this work were rectilinear. Furthermore, the authors did not observe the bouncing motion mentioned by Tsao and Koch (1997) and computed by DeBisschop et al. (2002) as well as by Norman and Miksis (2005a). It is likely that in the present work, the bubble volume was too large and the inclination of the solid wall was too small to provoke the bouncing motion. In water, propanediol, glycerine and their "solutions", the authors did not observe the break-up of the bubbles. However, in pure isopropanol as well as in its solutions (numbers 5 and 6, Table 2) bubble rupture occurred frequently at high volume when the bubble was released by the inverted cup method. Sometimes a large bubble ($V > 7$ cm^3) ruptured during its ascension under the inclined wall. This phenomenon may be explained by the fact that the surface tension of the isopropanol is the lowest among the modelling liquids used in our experiments.

3. Results and discussion

3.1. Effect of the fluid properties on the bubble shape

In this work, the bubble shape is basically characterized in the plane of the solid surface. The different geometrical parameters used are shown in Fig. 2. The instantaneous aspect ratio is defined by

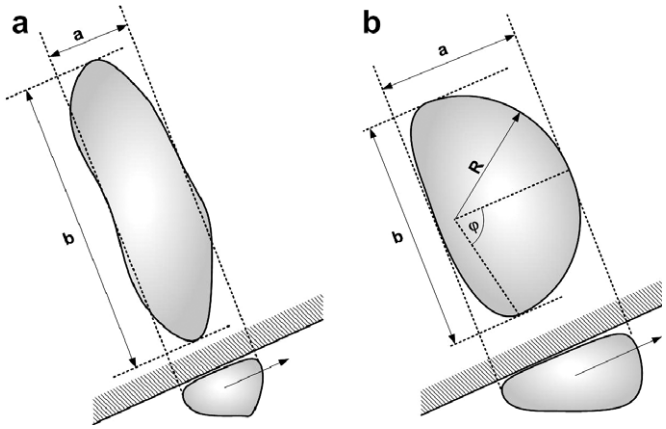

Fig. 2. Illustration of the different geometrical parameters used to describe the bubble shape: (a) deformable bubble, (b) semi-rigid bubble.

$$r(t) = \frac{b(t)}{a(t)}. \tag{7}$$

In the analysis of the results the average values of $r(t)$ will be used. Although the mean aspect ratio does not describe the shape of the bubble in detail, it gives an idea about some basic tendencies of the shape evolution, like the transition from a longitudinally elongated form ($r < 1$) into a transversely elongated one ($r > 1$). Generally, for semi-rigid bubbles (Fig. 2b), it was found that the frontal part of the moving bubble has a nearly perfect circular shape. Then, two parameters of the circular segment such as the radius of curvature R and the central angle φ were used to characterize the geometry of the bubble nose. The shape in the vertical section through the axis of motion (longitudinal plane or vertical plane) is described in the following lines. In most of the cases, the contour of the bubbles in the vertical section is convex. However, in certain circumstances, the curvature of the contour varies, convex and concave segments coexist. Under such conditions, the thickness of the front of the bubble is bigger than that of the rear part. Fortin et al. (1984) observed this phenomenon for very large bubbles moving under a slightly inclined surface. The interface deformation is nearly steady and the bubble front (the so-called "nose") may reach a thickness of 2 cm as shown in Fig. 5b. In our interpretation, the formation of a deeper, thicker gas-head at the nose of big gas pockets in motion is analogous to the formation of hydraulic jumps in free surface flows.

Fig. 3 shows the strong effects of the liquid properties on the bubble shape for different volumes at an inclination of 4°. The different shapes presented in this figure are observed in the pure liquids. The bubble movement is directed to the right. The four nominal bubble volumes presented in Fig. 3 correspond to one sub-regime introduced in an earlier work (Perron et al., 2006a). Those sub-regimes have been observed in water. The smallest volume corresponds to the *semi-rigid bubble* while the second one is termed the *oval oscillating bubble*. The bubble volumes of 4.0 cm^3 and 7.0 cm^3 correspond to the *deformable bubble* and the *bulged bubble* sub-regimes, respectively. Besides the dominant tendencies shaping the bubbles into approximately round, oval or elongated forms, there are secondary effects that result in ripples, protuberances as well as undulations. The complexity of bubble shape is a result of many interacting factors like surface tension, gas pressure, hydrodynamic forces, etc. In the case of large bubbles, there is a nonlinear interaction between bubble shape and hydrodynamic forces. Certain velocity and vorticity distributions provoke a deformation of the bubble interface which in turn will change the flow pattern around the bubble. These nonlinear interactions are responsible for the oscillations in the shape.

For the bubbles of 0.5 cm^3, the strong influence of the liquid on the dynamical bubble shape is shown in the first column of Fig. 3 as well as in Fig. 4a which presents the instantaneous aspect ratio of the moving bubbles as function of their position under the plate in order to homogenise the time scale. In water, the bubble has a nearly circular shape with a slightly higher radius of curvature at its front. The mean aspect ratio r is 1.36 and the amplitude of fluctuations is weak. The bubble of 0.5 cm^3 in isopropanol presents a more elongated shape in the direction perpendicular to the bubble movement with a mean value of r equals to 4.11. Furthermore, the

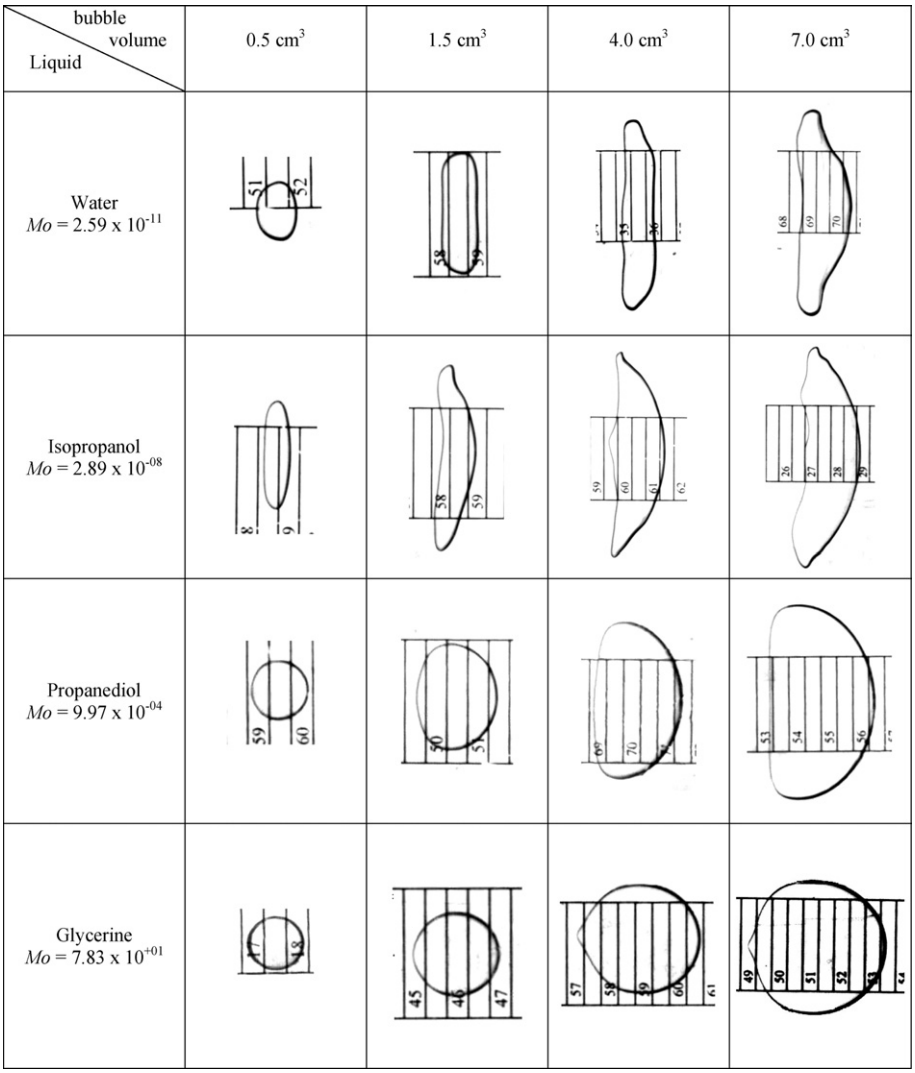

Fig. 3. Dynamical bubble shapes for different bubble volumes in various pure liquids at a surface inclination of 4°. The bubble movement is directed to the right and the shapes are characterized by their contour in the plane of the solid surface.

amplitude of fluctuations is higher than in the case of the previous bubble in water. The oscillations show periodic behaviour. The fluctuations of $r(t)$ for the moving bubbles of 0.5 cm^3 through propanediol and through glycerine are strongly attenuated and the bubble shape is circular. For the former, the average values of the aspect ratio are 1.05 while for the later, $r = 0.97$. The bubble interface in the vertical plane behaved as if it were rigid for all bubbles having a volume of 0.5 cm^3. The aspect ratio of the bubble of 1.5 cm^3 in water oscillates periodically around a mean value of the aspect ratio of 3.09. There is no hydraulic jump visible in the vertical section. The corresponding bubble in isopropanol is more deformable and the shape oscillations are still periodic with an average value $r = 4.93$. In the vertical plane, there is a non-steady deformation – a hydraulic jump – as shown in Fig. 5a. In high-Morton-number liquids, the bubble shape is strongly different. The bubble in propanediol shows an ellipsoidal cap shape while the one in glycerine still presents a circular shape. As we will see in the next section, an arbitrary distinction will be done between the high- and low-Morton-number liquids based on the behaviour of the terminal Froude number as function of the Bond number. The average values of r are 1.34 for the former and 0.95 for the latter (Fig. 4b). The axis of the bubble in the direction of the movement through glycerine is slightly longer than the axis perpendicular to it. This elongation is due to the

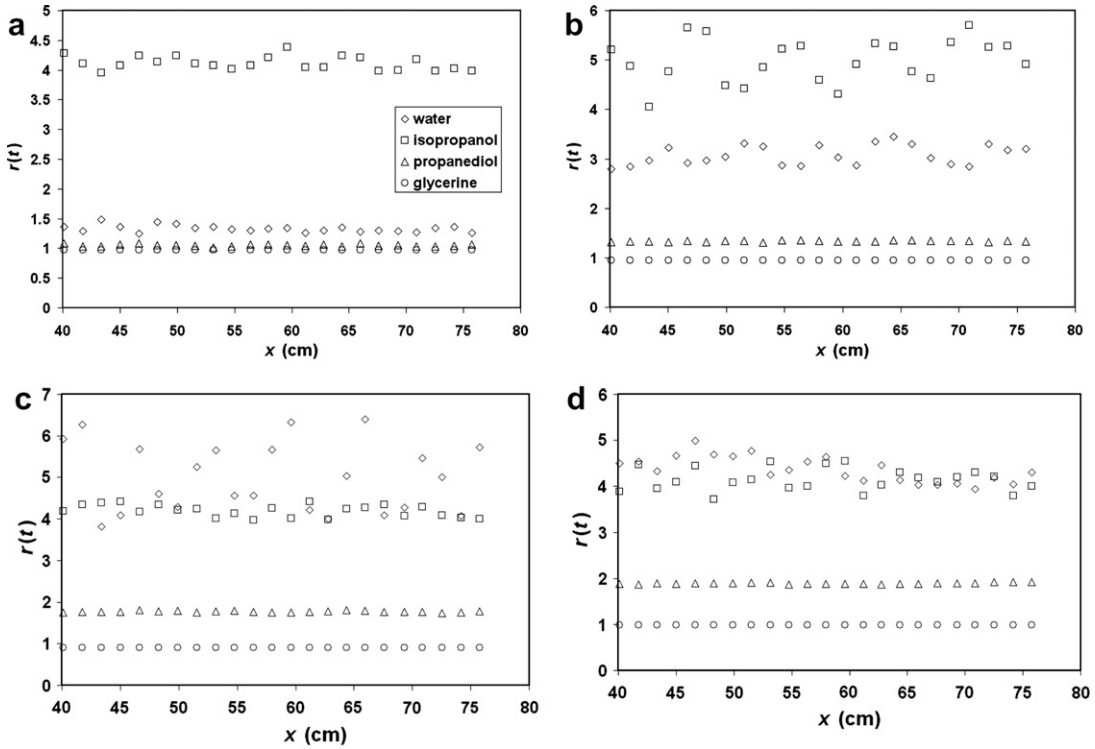

Fig. 4. Instantaneous aspect ratio for moving bubbles through different liquids at an inclination of 4°: (a) 0.5 cm^3, (b) 1.5 cm^3, (c) 4 cm^3 and (d) 7 cm^3. The symbols used for the different pure liquids are presented in (a).

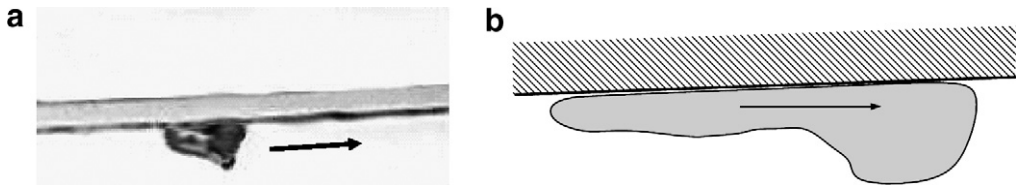

Fig. 5. Side view of a deformable bubble moving towards the right: (a) a picture of a non-steady interface deformation, called hydraulic jump, is observable for intermediate bubble size in low-Morton-number liquids; (b) a schematic representation of a nearly steady hydraulic jump for very large bubbles as observed by Fortin et al. (1984).

formation of a small 'tail' at the rear part of the bubble. The 'tail' is more visible at higher bubble volumes. In the longitudinal plane, the interface contour is rigid. The bubble of 4.0 cm^3 in water is characterized by strong amplitude of fluctuations around a mean value of 5.06. In the vertical plane, there is a non-steady hydraulic jump. The corresponding bubble in isopropanol forms a kind of boomerang shape always with a deformation of the interface contour in the vertical longitudinal section. The mean value of the aspect ratio is 4.20 and the bubble shape is more stable than the previous one of 1.5 cm^3. In viscous liquids, there is no major change in the characteristic bubble shape anymore. However, in propanediol, a weak tendency to decrease the curvature at the rear part of the bubble with increasing volume may be observed. In other words, the rear part tends to be straightened at intermediate and large volumes. The aspect ratio of the bubbles through the propanodiol and the glycerine is 1.77 and 0.90, respectively. The bubble of 7 cm^3 in water forms a *bulged bubble* with a mean aspect ratio of 4.45. The amplitude of the shape oscillations is weaker than for the previous bubble of 4 cm^3. This tendency (attenuation of the shape oscillations as the Bond number increases) observed in low-Morton-number liquids may be similar to the results of Norman and Miksis (2005a) who mentioned that when the bubble reached a near spherical-cap shape, the amplitude of oscillation damps out. The

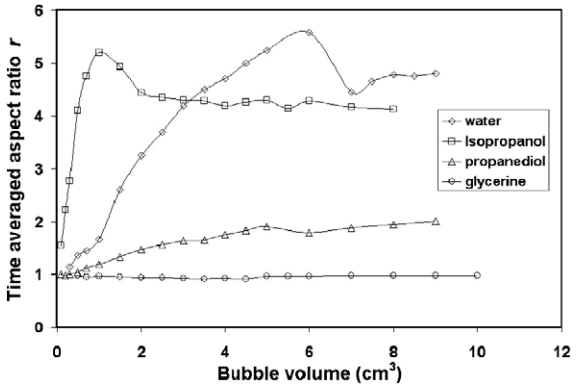

Fig. 6. Time-averaged aspect ratio as function of the bubble volume for the four different pure liquids at a surface inclination of 4°.

characteristic shape of the bubble in isopropanol is the same as that for 4 cm^3. The aspect ratios for the bubbles of 7 cm^3 moving through the isopropanol, propanediol and glycerine are 4.14, 1.91 and 0.98, respectively.

Fig. 6 shows the time-averaged aspect ratio for the four pure liquids as function of the bubble volume for an inclination angle of 4°. An evident observation is that all the four curves reach a plateau of nearly constant r at different values of the bubble volume. In two cases the curves are monotonous while for water and isopropanol the plateau is preceded by a maximum. The volume value at which the plateau is reached for each liquid is not a monotonous function of the Morton number. However, the nearly constant value of r obtained in each curve seems to be described by a monotonous relation of the Mo. In glycerine, r is independent of V and its value is almost 1. Fig. 7 shows the radius of curvature R at the bubble nose and the angle φ (see Fig. 2b) as function of the volume for bubbles moving through the high-Morton-number liquids at a slope of 4°. These two parameters characterize the circular segment of the interface contour in the plane. In Fig. 7a, R increases monotonously with the bubble volume while the angle φ decreases rapidly from 180° to an asymptotic value of 140°. The latter asymptotic value is denoted by φ^* in the following paragraphs. For bubbles moving through propanediol, at low bubble volume there is a weak increase of the aspect ratio until a value of 5 cm^3 (Fig. 6). At this value, r reaches a nearly constant value of 1.90. The circular shape of the interface contour for intermediate bubbles ($V > 3$ cm^3) is restricted to an angle of 60° from the bubble nose (Fig. 7b). The decrease of the central angle φ with the bubble volume is more drastic than that observed in glycerine. The radius of curvature increases almost linearly with the bubble volume for both viscous liquids. The rate of increase of R is higher in propanediol than in glycerine. For instance, for the same bubble volume of 9 cm^3, R reaches a value of 4.31 cm for the former and 2.54 cm for the latter. In low-Morton-number liquids, the trend of the curves is markedly

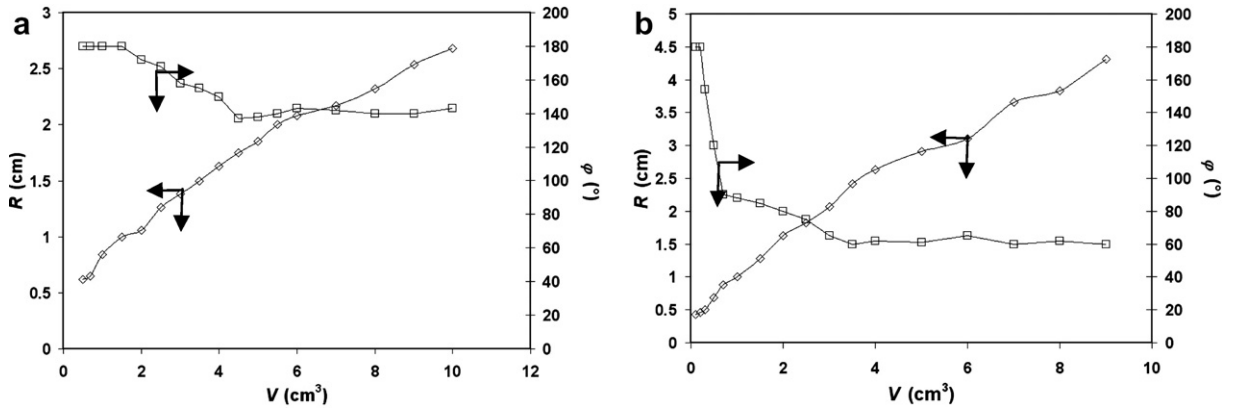

Fig. 7. Radius of curvature at the bubble nose R and the angle φ as function of the bubble volume for two different liquids at a surface inclination of 4°: (a) glycerine and (b) propanediol.

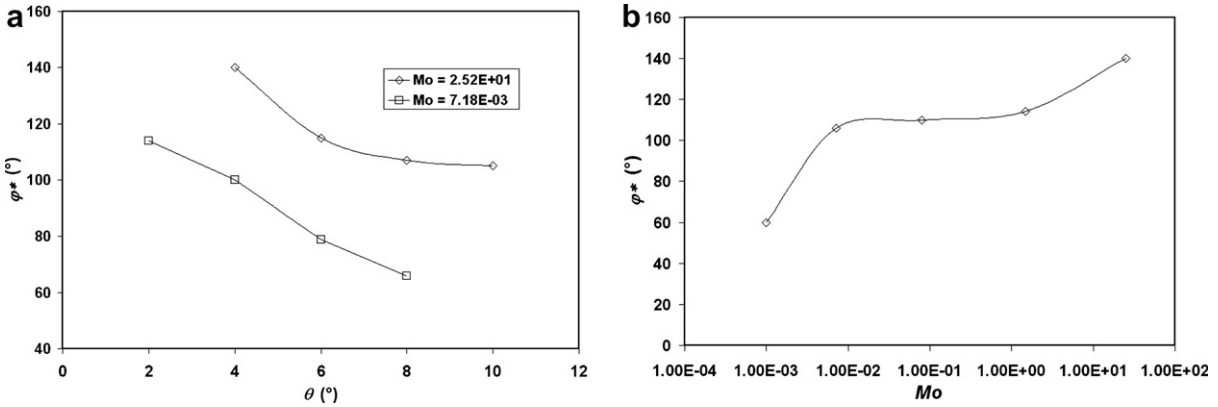

Fig. 8. (a) Variation of φ^* as function of the solid surface inclination angle and (b) influence of the Morton number on the value of φ^* for an inclination of 4°.

different. For bubbles in water, there is initially a growth of the aspect ratio as the bubble volume is increased. At $V = 6\ \mathrm{cm}^3$, the maximal value of 5.58 is reached. A further increase of the bubble volume provokes first a sharp decrease followed by a slight increase up to an almost constant value of 4.80. As it shown by Perron et al. (2006a), the decrease corresponds to the beginning of the *bulged bubble* sub-regime dominated principally by inertia. In isopropanol, the tendency of the curve is the same than in water. The major difference is the sharp increase of r at low bubble volumes. The marked increase of r at low bubble volumes may reflect the fact that the surface tension of the isopropanol is about three times lower than the one of water.

Fig. 8a shows the variation of the asymptotic value of the central angle describing the circular shape of the bubble nose φ^* as function of the inclination angle of the solid surface θ for two different high-Morton-number liquids. For both liquids, φ^* decreases with the inclination angle. For $Mo = 2.52 \times 10^{+01}$, the influence of θ is stronger at low inclination angles while for $Mo = 7.18 \times 10^{-03}$, the rate of the diminution slows down, tending to a nearly constant value. Fig. 8b presents the effect of the Morton number on the asymptotic value of the central angle for the high-Morton-number liquids at a surface inclination angle of 4°. The increase with Mo is not monotonous. There are two sharp increases of φ^* in the Morton number range from 9.97×10^{-04} to $2.52 \times 10^{+01}$. Between these regions, there is a zone where φ^* increases slightly with Mo. The same behaviour has been observed for different surface inclination angles studied in the present work.

To summarize, the strong influence of the liquid properties on the characteristic bubble shape has been shown through several parameters such as the aspect ratio as well as the angle φ and the radius R of the circular front section for the high-Morton-number liquids. On the other hand, it is difficult to establish a global correlation between the average aspect ratio as function of the bubble volume and the Morton number for a wide range of the latter. This is due to the non-monotonous variation of certain variables as function of the Mo. For instance, the initial rate of increase of the aspect ratio with the bubble volume varies non-monotonously with the Mo at low bubble volumes. Nevertheless, some parameters such as the plateau values of the aspect ratio tend to increase with the Morton number. Furthermore, in the high-Morton-number liquids, the value of the asymptotic value of the central angle φ^* tends to increase with the Morton number. In other words, the bubble shape in the plane of the surface tends to be 'more circular' with increasing Mo. In Section 3.2, the influence of the liquid properties on the bubble terminal velocity is studied in detail.

3.2. Effect of the liquid properties on the terminal velocity

In Section 3.1, it has been shown that the working liquid has a strong effect on the characteristic bubble shape. Then it is also expected that the liquid plays an important role on the bubble terminal velocity. The liquids used were pure propanediol and isopropanol as well as their aqueous solutions. There was also glycerine used at different temperatures. Fig. 9 shows the bubble terminal velocity as function of the equivalent diameter d for an inclination of 4°. In Fig. 9d, the data for water ($Mo = 2.59 \times 10^{-11}$) are presented again

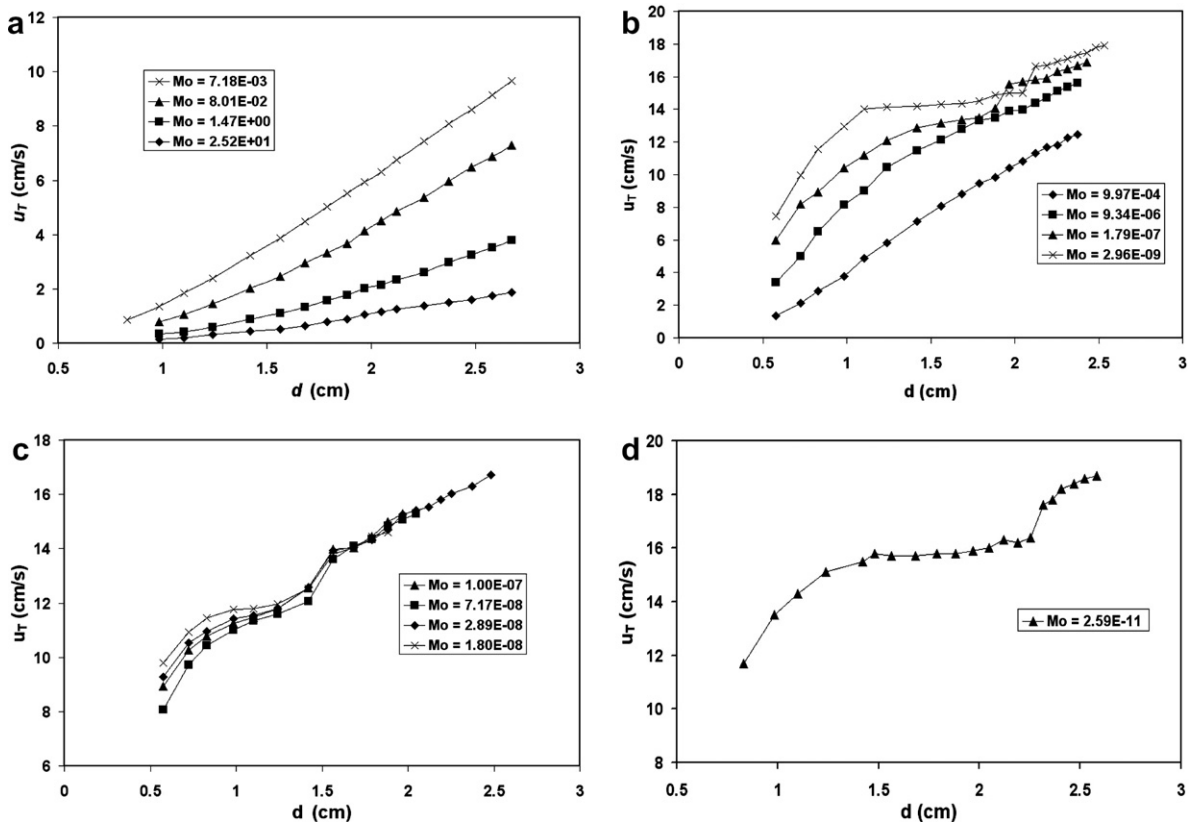

Fig. 9. Raw data of the terminal velocity as function of the equivalent diameter for different liquids at an inclination angle of 4°: (a) glycerine at different temperatures; (b) propanediol–water solutions; (c) isopropanol–water solutions and (d) water.

(Perron et al., 2006a) in order to compare the general tendency of the curves. In the water, the increase of the terminal velocity with the bubble volume is not monotonous. The authors identified four bubble sub-regimes each characterized by a specific bubble shape. At small equivalent diameters d, there is the *semi-rigid bubble* sub-regime followed by the *oval-oscillating bubble* sub-regime. At intermediate bubble volumes, it is the *deformable bubble* sub-regime and the terminal velocity is almost independent of the bubble volume. When the bubble volume becomes large enough to form a shape like a boomerang, u_T becomes function again of d and increases with it. The bubble with this specific shape is called *bulged bubble*. For the glycerine solutions (Fig. 9a), the behaviour of the curves is simple compared to the other liquids; u_T increases monotonously with d. At a given bubble volume (given d), the terminal velocity increases when the Morton number is decreased. In the propanediol solutions (Fig. 9b), the curves with a relatively high value of Mo present the same behaviour than glycerine while the curves with a low value of Mo show similarities with the water. Except the transition zone from the *deformable bubble* to the *bulged bubble* sub-regimes, u_T decreases with Mo at a given bubble volume. As it is shown in Table 2, the range of the Morton number describing the four isopropanol solutions is narrow. However, the curves in Fig. 9c present some interesting phenomena. First, for low bubble volumes, the bubble dynamics is influenced by a small change in the Mo and the bubble terminal velocity is not a monotonous function of the Mo. Finally, the curves in the *bulged bubble* sub-regime converge to a single one even if there is difference in the values of the Morton number.

Figs. 10 and 11 show the raw data presented in Fig. 9 in a dimensional form. In the graphs, the Froude (Maxworthy, 1991) and the Bond numbers are defined by

$$Fr = \frac{u_T}{\sqrt{dg\sin\theta}}, \tag{8}$$

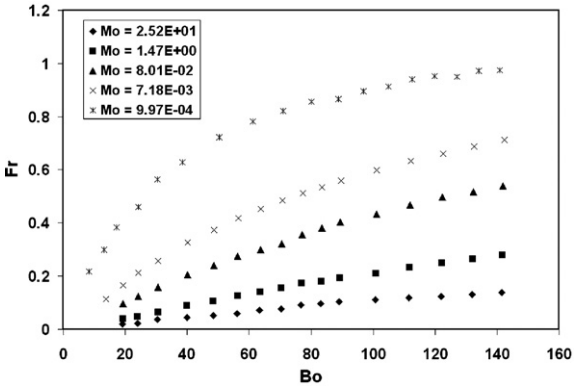

Fig. 10. *Fr* as function of *Bo* at an inclination angle of 4° for the high-Morton-number liquids.

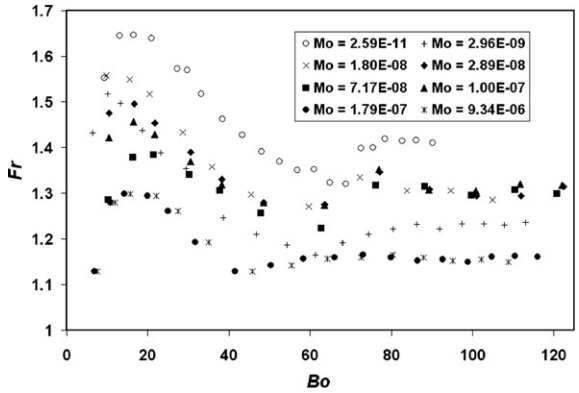

Fig. 11. *Fr* as function of *Bo* at an inclination angle of 4° for the low-Morton-number liquids.

where θ is the solid surface inclination angle and

$$Bo = \frac{\rho_L g d^2}{\sigma}, \tag{9}$$

respectively. The results are divided into two groups: the high- and low-Morton-number liquids (Figs. 10 and 11, respectively). The arbitrary distinction is inspired by Harper (1972) who considered the low-Morton-number liquids as those in which the C_d–*Re* curve has a minimum. In the present work, the latter liquids are those in which the *Fr*–*Bo* curve has a maximum at an inclination of 6°. For the high-Morton-number liquids (Fig. 10), the increase of the Froude number with the Bond number is monotonous. At an inclination of 4° and even at high *Bo*, the *Fr* still does not reach a nearly constant value. Furthermore, at a given Bond number, the Froude number increases when the Morton number decreases. In high-Morton-number liquids, the relation $Fr = Fr(Bo, Mo, \theta)$ including the Morton, Bond and Froude numbers as well as the inclination angle of the solid surface may describe the motion of a bubble under a slightly inclined surface in the wetting regime.

In low-Morton-number liquids (Fig. 11) the results are more difficult to interpret. First, for all the curves, the variation of *Fr* as function of the *Bo* is not monotonous. Second, beyond a value around 80 of the *Bo*, all the curves reach a nearly constant value of the Froude number. When *Fr* becomes independent of *Bo*, the *bulged bubble* sub-regime is reached. The latter corresponds to the well-known spherical-cap regime in an extended fluid (Maxworthy et al., 1996). Continuing the analogy, it is well known that in the inertial regime, the bubble motion through an infinite medium is independent of the liquid properties (Hartunian and Sears, 1957). In other words, all the curves corresponding to different Morton numbers converge to a single one in the spherical-cap regime. In our case the situation is more complex due to the presence of the wetting film. The

bubble motion is controlled on one hand by the flow around the lower bubble interface and on the other hand, by the viscous dissipation associated with the existence of the wetting film between the bubble and the solid plate. Indeed, as we can see in Fig. 11, the curves do not converge to a unique one. Furthermore the asymptotic values are not a monotonous function of the Morton number. For the isopropanol solution, the four curves converge to a unique value of the Froude number of around 1.3. This convergence may be due to the fact that the nature of the liquid is the same. Fig. 11 shows clearly that the combination of non-dimensional parameters $Fr = Fr(Bo, Mo, \theta)$ is not sufficient to describe the motion of a bubble moving under a slightly inclined solid surface for a wide range of the Morton number. First, the role of the Morton number on the bubble motion is difficult to interpret and second, a combination of the same non-dimensional parameters (Bo, Mo, θ) give two different values of the Froude number in the *bulged bubble* sub-regime. For instance, the asymptotic values for the propanediol solution $Mo = 1.79 \times 10^{-07}$ and the isopropanol solution $Mo = 1.00 \times 10^{-07}$ are 1.15 and 1.30, respectively. Recalling that the Froude number represents the ratio of inertial to gravity forces, it is likely that, from a dynamical point of view, the choice of Maxworthy (1991) (*Fr* being the dependent parameter) is not the best to described the bubble motion under an inclined plane when the Morton number varies largely. The results obtained in the present work suggest the use of the terminal Reynolds number as the dependent non-dimensional parameter to describe the motion of a bubble under an inclined solid plate. Fig. 12 shows the variation of the Reynolds number as function of the Bond number at an inclination angle of 4° for the whole set of liquids used in this work. With this combination of the non-dimensional parameters $Re = Re(Bo, Mo, \theta)$, the bubble motion may be clearly characterized and the role of the Morton number on the bubble dynamics can be illuminated. The variation of *Re* with *Mo* at a given Bond number is monotonous as shown in Fig. 13 and it decreases as the *Mo* increases. The same tendency has been observed at different inclination angles.

In order to facilitate the application of our findings to mathematical modelling of bubble laden flows, the results have been cast into an empirical correlation of the Reynolds number inspired by Angelino (1966):

$$Re = fBo^{g}, \tag{10}$$

where *f* and *g* are parameters which both depend upon the properties of the liquids and the inclination angle of the surface. Fig. 14 presents the values of those parameters for inclination angles of 2°, 4° and 6°. The correlations 10 and 11 are valid for $20 \leqslant Bo \leqslant 150$ in the whole range of the Morton number from 2.59×10^{-11} to $2.52 \times 10^{+01}$. The maximal deviation is around 5%. Recalling that the terminal velocity of a bubble moving under a solid plate is reached when the component parallel to the surface of the buoyancy force equals the drag force, the drag coefficient C_d can also be computed by

$$C_d = \frac{4}{3}\left(\frac{Bo^{3/2-2g}}{f^2 Mo^{1/2}}\right)\sin\theta \tag{11}$$

if all the terms in the relation $Re = Re(Bo, Mo, \theta)$ are known.

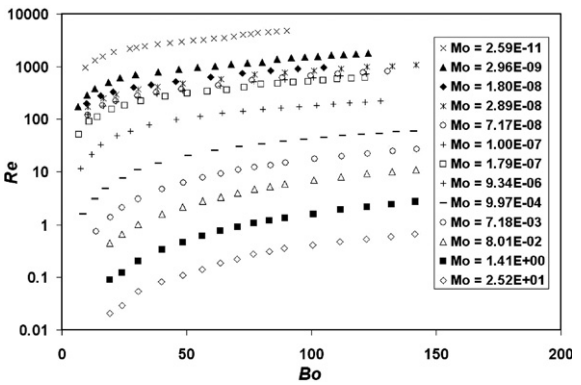

Fig. 12. Reynolds number as function of the Bond number at an inclination angle of 4° for the whole set of liquids used in this work.

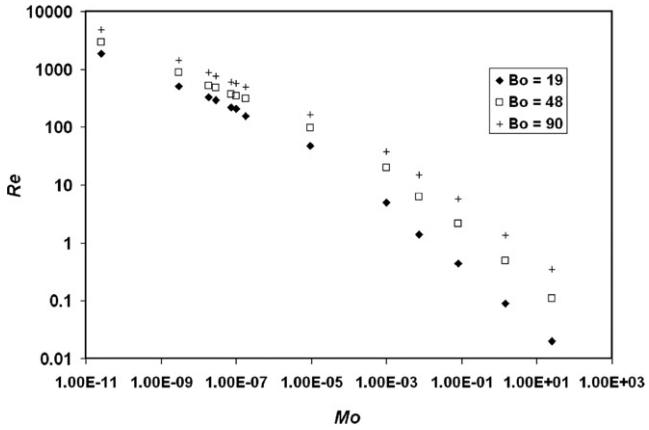

Fig. 13. Variation of the *Re* as function of the *Mo* for three different values of the Bond number at an inclination of 4°.

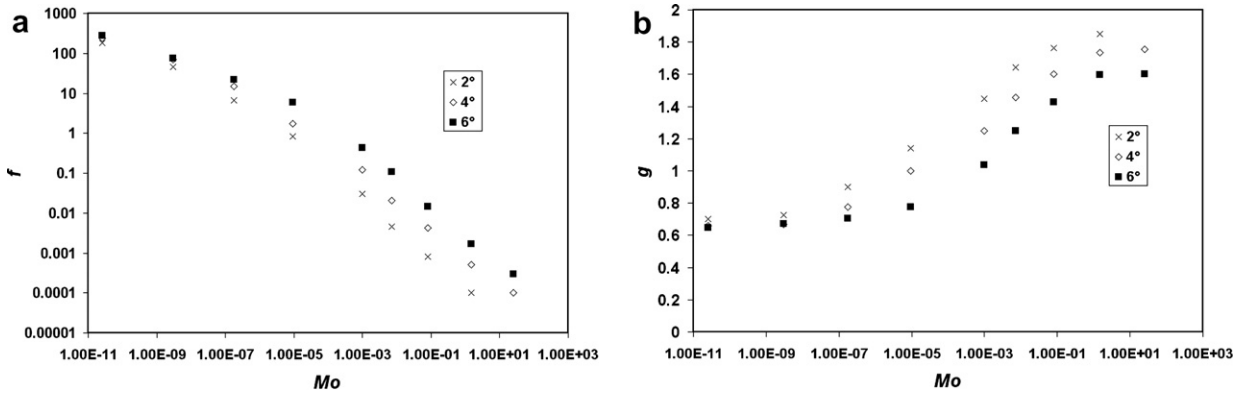

Fig. 14. Values of the parameters *c* and *d* used in expression (10) for three different inclination angles 2°, 4° and 6°.

To resume, in this subsection, the role of the Morton number on the bubble dynamics has been clarified with the appropriate choice of the dependent parameter. At a given Bond number, the Reynolds number decreases monotonously with the Morton number. Furthermore, an empirical correlation for the terminal *Re* has been given to facilitate the mathematical modelling of bubbly flow for different inclination angles. The choice of the terminal Reynolds number as the dependent parameter, may reflect the role of the wetting film in controlling the bubble motion. To improve the understanding of the momentum transfer between the bubble and the plate, the thickness of the wetting film must be known. To shed light on this issue, a multifiber optic sensor to measure the liquid film thickness has recently been developed by the authors (Perron et al., 2006b).

4. Conclusions

In this work, the influence of the liquid properties on the dynamical bubble shape as well as on the bubble terminal velocity has been studied in detail. All data reported here concern bubbles moving in the wetting regime, i.e. when there is a thin liquid film between the bubble interface and the solid surface. Air bubbles and different liquid (isopropanol, propanediol and glycerine) solutions were used in the two-phase gravity driven system. The solid surface was represented by a plate of Plexiglass. The Bond number covered the range from 10 to 150 and the surface inclination angles were varied from 2° to 6°. In the studied ranges, the results have shown that

- The effect of the liquid properties on the dynamical bubble shape is complex. The bubbles moving through low-Morton-number liquids are much deformable than those moving through high-Morton-number liquids. Indeed, the maximal values of the aspect ratio reach about 5 for the former and 2 for the latter. The variation of the aspect ratio with the bubble volume at a given inclination depends upon the liquid properties.
- In high-Morton-number liquids at a given surface inclination, the radius of curvature at the bubble front R increases monotonously with the bubble volume while the central angle φ, which characterizes the circular frontal section of the bubble interface contour in the plane of the solid, decreases sharply at low bubble volumes and reaches a nearly constant value at high volumes.
- The relation $Fr = Fr(Bo, Mo, \theta)$ does not describe unambiguously the motion of a bubble under a slightly inclined solid surface in a wide range of the Morton numbers. The choice of the terminal Reynolds number as dependent parameter allowed the clarification of the role of the Morton number on the bubble motion. At a given Bond number, the terminal Reynolds number of the bubble decreases monotonously with the Morton number.
- An empirical correlation $Re = Re(Bo, Mo, \theta)$ to support mathematical modelling of bubbly flows in the studied range of parameters has been given.

Acknowledgements

The first author gratefully acknowledges the support of the Fonds québécois de recherches sur la nature et les technologies (FQRNT) and that of the Conseil de Recherches en Sciences Naturelles et en Génie du Canada (CRSNG) in the form of post-graduate scholarships. The authors also express their thanks to Mr. Sylvain Desgagné and Mrs. Geneviève Desclaux for the technical assistance.

References

Angelino, H., 1966. Hydrodynamique des grosses bulles dans les liquides visqueux. Chem. Eng. Sci. 21, 541–550.

Antal, S.P., Lahey Jr., R.T., Flaherty, J.E., 1991. Analysis of phase distribution in fully developed laminar bubbly two-phase flow. Int. J. Multiphase Flow 17, 635–652.

Bhaga, D., Weber, M.E., 1981. Bubbles in viscous liquids: shapes, wakes and velocities. J. Fluid Mech. 105, 61–85.

DeBisschop, K.M., Miksis, M.J., Eckmann, D.M., 2002. Bubble rising in an inclined channel. Phys. Fluids 14, 93–106.

Fortin, S., Gerhardt, M., Gesing, A.J., 1984. Physical modelling of bubble behaviour and gas release from aluminum reduction cell anodes. TMS Light Met., 721–741.

Harper, J.F., 1972. The motion of bubbles and drops through viscous liquids. Adv. Appl. Mech. 12, 59–129.

Hartunian, R.A., Sears, W.R., 1957. On the instability of small bubbles moving uniformly in various liquids. J. Fluid Mech. 3, 27–47.

Maneri, C.C., Zuber, N., 1974. An experimental study of plane bubbles rising at inclination. Int. J. Multiphase Flow 1, 623–645.

Masliyah, J., Jauhari, R., Gray, M., 1994. Drag coefficients for air bubbles rising along an inclined surface. Chem. Eng. Sci. 49, 1905–1911.

Maxworthy, T., 1991. Bubble rise under an inclined plate. J. Fluid Mech. 229, 659–674.

Maxworthy, T., Gnann, C., Kürten, M., Durst, F., 1996. Experiments on the rise of air bubbles in clean viscous liquids. J. Fluid Mech. 321, 421–441.

Norman, C.E., Miksis, M.J., 2005a. Dynamics of a gas bubble rising in an inclined channel at finite Reynolds number. Phys. Fluids 17, 13.

Norman, C.E., Miksis, M.J., 2005b. Gas bubble with a moving contact line rising in an inclined channel at finite Reynolds number. Physica D 209, 191–204.

Perron, A., Kiss, L.I., Poncsák, S., 2006a. An experimental investigation of the motion of single bubbles under a slightly inclined surface. Int. J. Multiphase Flow 32, 606–622.

Perron, A., Kiss, L.I., Verreault, R., 2006b. A multifiber optic sensor to measure the liquid film thickness between a moving bubble and an inclined solid surface. Meas. Sci. Technol. 17, 1594–1600.

Tsao, H.K., Koch, D.L., 1997. Observations of high Reynolds number bubbles interacting with a rigid wall. Phys. Fluids 9, 44–56.

Weber, M.E., Alarie, A., 1986. Velocities of extended bubbles in inclined tubes. Chem. Eng. Sci. 41, 2235–2240.

Zukoski, E.E., 1966. Influence of viscosity, surface tension and inclination angle on motion of long bubbles in closed tubes. J. Fluid Mech. 25, 821–837.